PCCP

Accepted Manuscript




ROYAL SOCIETY OF CHEMISTRY

www.rsc.org/pccp

# Lithium cation conducting TDI anion-based ionic liquids

Leszek Niedzicki*[a], Ewelina Karpierz[a], Maciej Zawadzki[b], Maciej Dranka[a], Marta Kasprzyk[a], Aldona Zalewska[a], Marek Marcinek[a], Janusz Zachara[a], Urszula Domańska[b], Władysław Wieczorek[a]

## Table of contents entry

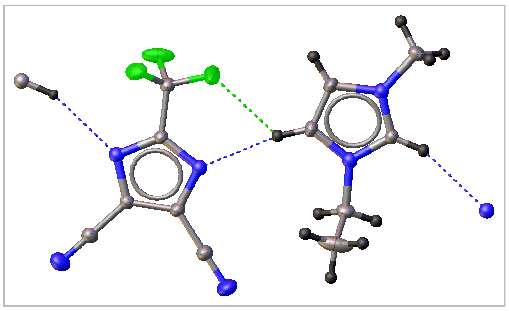

LiTDI salt in TDI-imidazole ionic liquids tested as lithium electrolytes shown high ionic conductivity and high lithium transference number.

## Abstract

In this paper we present the synthesis route and electrochemical properties of new class of ionic liquids (ILs) obtained from lithium derivate TDI (2-trifluoromethano-4,5-dicyanoimidazole) anion. ILs synthesized by us were EMImTDI, PMImTDI and BMImTDI, *i.e.* TDI anion with 1-alkyl-3-methylimidazolium cations, where alkyl meant ethyl, propyl and

* corresponding author, email: lniedzicki@ch.pw.edu.pl, phone: +48 22 234 7421, fax: +48 22 628 2741

[a] Warsaw University of Technology, Faculty of Chemistry, Department of Inorganic Chemistry and Solid State Technology, Noakowskiego 3, 00664 Warsaw, Poland

[b] Warsaw University of Technology, Faculty of Chemistry, Department of Physical Chemistry, Noakowskiego 3, 00664 Warsaw, Poland

butyl groups. TDI anion contains less fluorine atoms than $LiPF_6$ and thanks to C-F instead of P-F bond, they are less prone to emit fluorine or hydrogen fluoride due to the rise in temperature. Use of IL results in non-flammability, which is causing such electrolyte even safer for both application and environment.

Thermal stability of synthesized compounds was tested by DSC and TGA and no signal of decomposition was observed up to 250˚C. The LiTDI salt was added to ILs to form complete electrolytes. Structures of tailored ILs with lithium salt were confirmed by X-ray diffraction patterns. Electrolytes showed excellent properties regarding their ionic conductivity (over 3 mS $cm^{-1}$ at room temperature after lithium salt addition), lithium cation transference number (over 0.1), low viscosity and broad electrochemical stability window. Ionic conductivity and viscosity measurements of pure ILs are reported for reference.

## 1. Introduction

No doubt Li (ion) battery is one of the most emerging devices for energy storage.[1-3] While there are significant numbers of publications on the new lithium-ion cell electrode materials (or additions to those), very little attention have been devoted to new salts used in lithium electrolytes.

That was the reason of the concept of creating new anions for lithium ion batteries. The whole idea came from the transposition of the Hückel rule predicting the stability of the aromatic salt systems. One of the most common examples of this type of anions (sometimes called “Hückel anions”) is 4,5-dicyano-triazole (DCTA). This particular structure is completely covalently bonded and shows very stable 6π (or 10π electron if CN bonds are involved in calculations) configuration. LiDCTA was successfully tested in PEO matrices systems as a promising, improved electrolyte for rechargeable lithium batteries.[4] Unfortunately DCTA failed as a component of the EC/DMC (1:1) battery electrolyte.

Therefore, new "tailored" anions were studied by our group, which have been designed and investigated directly for application as lithium electrolytes in lithium-ion cells. Several patents and papers[5-9] were published before, describing details about synthesis, production, structure and electrochemical properties of perfluorinated anion based lithium salts. These new compounds showed thermal stability (over 250˚C, no aluminum corrosion and electrochemical stability up to 4.6 V) and transference number properties superior to the presently used lithium salts in electrolytes. Also the safety aspects of the pure lithium (2-trifluoromethano-4,5-dicyanoimidazole) LiTDI were published recently.[10]

So far these salts were studied as a component of solid or liquid electrolytes.[5-7] The present paper extends their use to ionic liquid (IL) based electrolytes.

Classical solvents in batteries (*e.g.* EC, DMC, PC) are usually toxic and flammable (volatile). The low vapor pressure of ILs has very important advantages compared to other so called volatile organic chemicals (VOCs). Therefore ILs are neither flammable nor explosive and a risk of prolonged pollution into the air is substantially reduced.[11,12] In consequence, new solvents, such as ILs, considered as alternative technologies offer minimal evaporation into the atmosphere allowing simple recycling and reuse. Using simple syntheses as proposed in our manuscript is a good way of limitation of any unwanted byproducts and wastes. These are the clear environmental aspects of such type of electrolytes. It should be definitely mentioned that ILs offer huge environmental advantage when considering them as so-called "green chemistry" compounds in battery industry. One of the principles of green chemistry put special attention to the new approach toward industrial procedures where any kind of wastes are not treated anymore simply as byproducts of the chemical processes so the simple synthesis route proposed here fulfill these requirements.

Richness of structural variations and chemistry behavior[13,14] makes ILs attractive candidates for many applications.[15] The interest in the ILs as electrolytes for the lithium (ion) batteries is increasing with the popularity of lithium batteries as energy storage for everyday use and with social pressure on green technologies development.[16] The reason is obvious: ILs offer high conductivity, non-flammability, wide electrochemical and thermal stability windows.[17] However, up till now, there have been many disadvantages of these new materials. One of them has been large decrease of conductivity with the addition of lithium salt to IL, which limits possible charge and discharge rate of cell containing such an electrolyte. Other disadvantages have included melting point higher than room temperature, which constrains applications of such materials to a limited number. A very low lithium cation transference number (less than 0.1) that impacts charge-discharge cycle efficiency has been also an issue.

In this paper we introduce for the very first time the new class of ILs potentially able (due to its atomic and electronic structure) to overcome majority of existing electrochemical disadvantages of this kind of materials. Also a low content of fluorine in proposed electrolyte composition might create a new added value of “green” aspect of ILs.

## 2. Experimental

### 2.1. Synthesis

#### 2.1.1. LiTDI

Lithium (4,5-dicyano-2-(trifluoromethane)imidazole) synthesis route was described previously.[18] Figure 1 shows the structural formula of LiTDI and all subsequently obtained ILs.

### 2.1.2. 1-Ethyl-3-methylimidazolium 4,5-dicyano-2-(trifluoromethyl)imidazolide (EMImTDI)

2.53 g 1-Ethyl-3-methylimidazolium chloride (as received, IoLiTec 98%)(0.0173 mol) in 10 ml of dichloromethane was added to a solution of 3.31 g lithium 4,5-(dicyano)-2-(trifluoromethyl)imidazol-1-ide (synthesized)(0.0172 mol) in 10 ml of water. Mixture was stirred at room temperature for 4 h and was left for separation of phases for 6 h. After that phases were separated by draining. Water phase was extracted with 10x8 ml of dichloromethane (until water phase was colorless). Then organic phase was extracted with 2x4 ml of water (removal of residual lithium chloride). Solvents were removed *in vacuo* and product was further dried under vacuum at 80°C for 12 h. Thus, we obtained 1-ethyl-3-methylimidazolium 4,5-dicyano-2-(trifluoromethyl)imidazolide (5.00 g, 97.9%).

$M$ = 296.25 g mol$^{-1}$; $T_m$ = 334.16 K; $\Delta H_m$ = 52.84 kJ mol$^{-1}$; $T_g$ = 174.84 K; $\Delta C_p$ = 280 J mol$^{-1}$ K$^{-1}$

Elemental analysis: Found: C, 49.0; N, 28.3; H, 4.0. Calc. for $C_{12}H_{11}N_6F_3$: C, 48.7; N, 28.3; H, 3.7%.

$^1$H NMR: $\delta_H$(400 MHz; d$_6$-Acetone; Me$_4$Si): 1.561 (3 H, t, $^3J_{HH}$ = 7.2 Hz, N-CH$_2$C*H*$_3$), 4.061 (3 H, s, N-CH$_3$), 4.403 (2 H, q, $^3J_{HH}$ = 7.2 Hz, N-C*H*$_2$CH$_3$), 7.734 (2 H, d, $^3J_{HH}$ = 28.8 Hz, N-C*H*C*H*-N), 9.066 (1 H, s, N-CH-N).

$^{13}$C NMR: $\delta_C$(100 MHz; d$_6$-Acetone; Me$_4$Si): 15.475, 36.580, 45.710, 116.056, 120.052, 123.056, 124.739, 137.002, 148.844, 206.468.

### 2.1.3. 1-Methyl-3-propylimidazolium 4,5-dicyano-2-(trifluoromethyl)imidazolide (PMImTDI)

18.20 g 1-Methyl-3-propyllimidazolium chloride (as received, IoLiTec 98%)(0.1133 mol) in 100 ml of water was added to a solution of 24.03 g lithium 4,5-(dicyano)-2-

(trifluoromethyl)imidazol-1-ide (synthesized)(0.1270 mol) in 100 ml of water. Mixture was stirred in room temperature for 4 h, after which 100 ml of dichloromethane was added and phases were separated. Water phase was extracted with 50 ml of dichloromethane. Then organic phase was extracted with 10x25 ml of water (removal of residual lithium chloride). Solvents were removed *in vacuo*, and product was further dried under vacuum at 80°C for 24 h. Thus, we obtained 1-methyl-3-propylimidazolium 4,5-dicyano-2-(trifluoromethyl)imidazolide (30.16 g, 85.8%).

$M$ = 310.28 g mol$^{-1}$; $T_m$ = 286.85 K; $\Delta H_m$ = 28.09 kJ mol$^{-1}$; $T_g$ = 203.81 K; $\Delta C_p$ = 246 J mol$^{-1}$ K$^{-1}$

Elemental analysis: Found: C, 50.0; N, 26.9; H, 4.2; Calc. for $C_{13}H_{13}N_6F_3$: C, 50.3; N, 27.1; H, 4.2%.

$^1$H NMR: $\delta_H$(400 MHz; $d_6$-Acetone; $Me_4Si$): 0.943 (3 H, t, $^3J_{HH}$ = 7.2 Hz, $CH_2CH_3$), 1.981 (2 H, hex, $^3J_{HH}$ = 7.2 Hz, $CH_2CH_2CH_3$), 4.067 (3 H, s, N-$CH_3$), 4.309 (2 H, t, $^3J_{HH}$ = 7.2 Hz, N-$CH_2CH_2$), 7.720 (2 H, d, $^3J_{HH}$ = 19.2 Hz, N-CHCH-N), 9.068 (1 H, s, N-CH-N).

$^{13}$C NMR: $\delta_C$(100 MHz; $d_6$-Acetone; $Me_4Si$): 10.598, 23.915, 36.565, 51.853, 115.942, 119.954, 123.260, 124.663, 137.100, 148.749, 206.892.

### 2.1.4. 1-Butyl-3-methylimidazolium 4,5-dicyano-2-(trifluoromethyl)imidazolide (BMImTDI)

6.38 g 1-Butyl-3-methylimidazolium chloride (as received, IoLiTec 98%)(0.0365 mol) in 100 ml of dichloromethane was added to a solution of 7.70 g lithium 4,5-(dicyano)-2-(trifluoromethyl)imidazol-1-ide (synthesized)(0.0401 mol) in 100 ml of water. Mixture was stirred in room temperature for 4 h, after which phases were separated. Water phase was extracted with 10x10 ml of dichloromethane. Then organic phase was extracted with 2x5 ml water (removal of residual lithium chloride). Solvents were removed *in vacuo* and product

was further dried under vacuum at 80°C for 12 h. Thus, we obtained 1-butyl-3-methylimidazolium 4,5-dicyano-2-(trifluoromethyl)imidazolide (10.14 g, 85%).

$M$ = 324.30 g mol$^{-1}$; no $T_m$; $T_g$ = 203.63 K; $\Delta C_p$ = 311 J mol$^{-1}$ K$^{-1}$

Elemental analysis: Found: C, 51.8; N, 25.8; H, 4.6; Calc. for $C_{14}H_{15}N_6F_3$: C, 51.8; N, 25.9; H, 4.6%.

$^1$H NMR: $\delta_H$(400 MHz; $d_6$-Acetone; $Me_4Si$): 0.877 (3 H, t, $^3J_{HH}$ = 7.2 Hz, $CH_2CH_3$), 1.302 (2 H, hex, $^3J_{HH}$ = 7.6 Hz, $CH_2CH_2CH_3$), 1.809 (2 H, tt, $^3J_{HH}$ = 7.2 Hz, $^3J_{HH}$ = 7.6 Hz, $CH_2CH_2CH_2$), 3.943 (3 H, s, N-$CH_3$), 4.152 (2 H, t, $^3J_{HH}$ = 7.2 Hz, N-$CH_2CH_2$-), 7.375 (2 H, m, N-C*H*C*H*-N), 9.025 (1 H, s, N-CH-N).

$^{13}$C NMR: $\delta_C$(100 MHz; $d_6$-Acetone; $Me_4Si$): 13.427, 19.759, 32.477, 36.557, 50.147, 115.950, 119.954, 123.268, 124.648, 137.085, 148.756, 206.816.

### 2.2. Salt characterization

Salts were characterized with differential scanning calorimetry (DSC) on TA Instruments Q200DSC apparatus and with thermogravimetric analysis (TGA) on TA Instruments Q600SDT apparatus. Heating rate in both cases was equal to 10 K·min$^{-1}$.

$^1$H NMR, $^{13}$C NMR and $^{19}$F NMR experiments were performed on Varian Gemini 200. $^1$H shifts are reported relative to TMS ($\delta$ = 0), $^{13}$C chemical shifts are reported relative to $CD_3CN$ ($\delta$ = 1.3). The $^{19}$F shifts are described with $CFCl_3$ as the reference ($\delta$ = 0).

Elemental analysis was conducted by combustion method with PerkinElmer 2400 series II CHNS/O Elemental Analyzer, using imidazole as reference sample, while working in CHN mode. Argon carrier gas was used, providing <0.4 % accuracy and <0.3 % precision. Three samples of 10 mg were used for measurement and results were averaged.

Trace moisture content of below 50 ppm level was determined with Karl Fischer titration method. Chloride content of below 20 ppm level was determined using potentiometric method.

### 2.3. X-ray crystallography

Selected single crystals were mounted in inert oil and transferred to the cold gas stream of the diffractometer. Diffraction data were measured at 100(2) K with graphite-monochromated Mo$K_\alpha$ (EMImTDI) or mirror monochromated Cu$K_\alpha$ (LiTDI-PMImTDI and LiTDI-BMImTDI) radiation on the Oxford Diffraction Gemini A Ultra diffractometer. Cell refinement and data collection as well as data reduction and analysis were performed with the CRYSALIS$^{PRO}$.[19] The structures were solved by direct methods with SHELXS−97.[20] Full-matrix least-squares refinement method against $F^2$ values were carried out by using the SHELXL−97[20] and OLEX2[21] programs. All non hydrogen atoms were refined with anisotropic displacement parameters. Hydrogen atoms were added to the structure model at geometrically idealized coordinates and refined as riding atoms. Crystal data and structure refinement parameters are given in Supplemental Table 1 (ESI).

**Crystal Data** for **EMImTDI (1)**: $C_{12}H_{11}F_3N_6$ ($M$ =296.27): triclinic, $P\bar{1}$ , $a$ = 8.63283(15) Å, $b$ = 8.86281(12) Å, $c$ = 10.25772(13) Å, $\alpha$ = 87.4723(11)°, $\beta$ = 78.8034(13)°, $\gamma$ = 66.0794(15)°, $V$ = 703.24(2) Å$^3$, $Z$ = 2, $\mu$(Mo $K\alpha$) = 0.119 mm$^{-1}$, $D_{calc}$ = 1.399 g/cm$^3$, 111869 reflections measured ($7.24 \leq 2\Theta \leq 58.98$), 3902 unique ($R_{int}$ = 0.0237). The final $R_1$ was 0.0408 ($I>2\sigma(I)$) and $wR_2$ was 0.1090 (all data).

**Crystal Data** for **LiTDI-PMImTDI (2)**: $C_{19}H_{13}F_6LiN_{10}$ ($M$ =502.33): triclinic, $P\bar{1}$ , $a$ = 8.28368(13) Å, $b$ = 11.45842(18) Å, $c$ = 12.57923(20) Å, $\alpha$ = 74.9663(14)°, $\beta$ = 77.5238(13)°, $\gamma$ = 78.6965(13)°, $V$ = 1113.43(3) Å$^3$, $Z$ = 2, $\mu$(Cu $K\alpha$) = 1.157 mm$^{-1}$, $D_{calc}$ = 1.498 g/cm$^3$, 60286 reflections measured ($7.38 \leq 2\Theta \leq 133.34$), 3923 unique ($R_{int}$ = 0.0330). The final $R_1$ was 0.0275 ($I>2\sigma(I)$) and $wR_2$ was 0.0711 (all data).

**Crystal Data** for **LiTDI-BMImTDI (3)**: $C_{20}H_{15}F_6LiN_{10}$ ($M$ =516.36): triclinic, $P\bar{1}$ , $a$ = 8.42410(11) Å, $b$ = 11.66815(17) Å, $c$ = 12.85431(18) Å, $\alpha$ = 73.0547(13)°, $\beta$ = 74.4505(12)°, $\gamma$ = 76.7560(12)°, $V$ = 1148.67(3) Å$^3$, $Z$ = 2, $\mu$(Cu $K\alpha$) = 1.137 mm$^{-1}$, $D_{calc}$ = 1.493 g/cm$^3$, 80701 reflections measured ($7.36 \leq 2\Theta \leq 133.4$), 4047 unique ($R_{int}$ = 0.0330). The final $R_1$ was 0.0298 ($I>2\sigma(I)$) and $wR_2$ was 0.0721 (all data).

### 2.4. Electrolytes characterization

Ionic conductivity measurements were performed using electrochemical impedance spectroscopy (EIS) in the nearest full 10°C over melting point up to 70°C temperature every 10˚C, over full range of concentration of LiTDI (pure IL, 0.0125, 0.025, 0.0375, 0.05, 0.075, 0.1, 0.125 and 0.15 mole fraction, the last being the maximum LiTDI solubility in all ILs). Electrolytes were placed into micro conductivity cells with cell constant equal to 0.5 cm$^{-1}$ which were put to a cryostat-thermostat system (Haake K75 with the DC50 temperature controller). All impedance measurements were carried out on the computer-interfaced multichannel potentiostat with frequency response analyzer option Bio-Logic Science Instruments VMP3 within 500 kHz-1 Hz frequency range with 10 point per decade and with 5 mV a.c. signal. Measurements were repeated with independently prepared samples to improve consistency of data, obtaining maximum differences of 5%.

Lithium cation transference numbers ($t_+$) were calculated using d.c. polarization method combined with a.c. impedance method introduced by Bruce and Vincent.[22] Details can be found in the Electronic Supplementary Information (ESI).

Linear sweep voltammetry (LSV) was used to investigate electrochemical stability window. Samples of electrolyte were sandwiched between lithium metal electrodes used as both counter and reference electrode and platinum electrode as a working electrode (Pt electrode surface was 0.1 cm$^2$). LSV was performed every time with 1 mV s$^{-1}$ scan rate at

ambient temperature for PMImTDI and BMImTDI and at 70°C in case of EMImTDI (due to its high melting point). Cyclic voltammetry results of neat ionic liquids are available in the supplemental materials.

Viscosity experiments were performed with Physica MCR301 Anton Paar Rheometer with CP40 cone tip and thermoelectric heat pump base for thermostating. Each time the 0.4 ml volume (excess) of the given electrolyte was used, thermostated with precision of 0.1°C at each temperature and measured in shearing rate of 10-1000 $s^{-1}$.

Symbols of mixture compositions will be used subsequently for clarity of text throughout descriptions of conductivity, viscosity and transference numbers results and discussion. The system of symbols is made as follows: first letter is the abbreviation of alkyl chain in the cation: E – ethyl, P – propyl, B – butyl; number means amount of thousandths of LiTDI molar fraction in the mixture of LiTDI and IL, *e.g.:* P0 means pure PMImTDI, E50 means $LiTDI_{0.05}EMImTDI_{0.95}$ and B125 means $LiTDI_{0.125}BMImTDI_{0.875}$. xMIm means any 1-alkyl-3-methylimidazolium cation.

## 3. Results and discussion

ILs exhibited the stability up to about 250°C, as seen on Figure 2. EMImTDI has the DTG decomposition onset at 253°C, PMImTDI at 251°C and BMImTDI at 247°C. Similar structures of cations and identical anion are probably the main reason for such small differences among them. These values are also very close to the LiTDI decomposition temperature (256°C). On the DTG curves three different regions can be observed. First one is a very slow one with the highest weight percent loss for EMImTDI. Second one is the main region of decomposition with very similar weight loss rate for all compounds - still EMImTDI takes the fastest weight loss. Subsequently, one more decomposition phase takes place which can be observed as a very narrow DTG signal for EMImTDI, as a widening of the main signal in case of PMImTDI and as a distinct one for BMImTDI. EMImTDI has the fastest weight

loss in the first two phases and negligible in third phase. Other two compounds have the same weight loss for the first two signals and noticeably different weight loss for the third phase – with BMImTDI taking the most significant weight loss in the last one. Observations described above are in the good agreement with findings by Chowdhury and Thynell.[23] Methyl elimination from xMIm cations is responsible for the initial weight loss of about 5% (first DTG peak integral), which is in concert with the methyl group share of IL weight. The main step is probably decomposition of the TDI anion[18] and the last step is assumed to be the elimination of alkyl group (ethyl, propyl or butyl, according to the cation). Thus, main products of decomposition are alkanes and their decomposition products (not known to be toxic), as well as TDI anion decomposition products. The latter are considered safer than $PF_6^-$ anion decomposition products, if only because of less fluorine atoms per molecule and no phosphor used. Hence, neither phosphines nor highly toxic fluorinated phosphines are produced, like in case of $LiPF_6$.

The electrochemical stability in case of EMImTDI and PMImTDI is sufficient for application in all state-of-the-art electrode materials for lithium-ion cells. Results of linear sweep voltammetry experiments performed on the 0.1 molar LiTDI mixtures with ILs are shown on Figure 3. Stability limits of these mixtures reach 4.6 V, 4.6 V and 4.0 V vs. Li for LiTDI-EMImTDI, LiTDI-PMImTDI and LiTDI-BMImTDI, respectively. The main influence here can be attributed to the anion – LiTDI salt has the 4.7 V stability boundary.[18] There is lack of other LSV signals down to 0.6, 0.8 and 0.6 V vs. Li in case of LiTDI-EMImTDI, LiTDI-PMImTDI and LiTDI-BMImTDI, respectively, showing good electrochemical stability and wide stability window.

Figure 4 shows the ionic conductivity plots comparison for pure IL and LiTDI-doped electrolytes. We can see that the highest ionic conductivity at the given temperature (70°C) has been measured for the EMImTDI and its mixtures with LiTDI. Pure IL reach ionic

conductivity of 28.9 mS $cm^{-1}$ (E0). After addition of salt conductivity value change to 18.6-18.7 mS $cm^{-1}$ in case of E25 and E37, 18.0 mS $cm^{-1}$ for E75 and as much as 20.3 mS $cm^{-1}$ for E150. To the best of our knowledge, such high (compared to pure IL) conductivities were never seen before in ILs after lithium salt addition, especially at such high molar fractions of lithium salt. Ionic conductivity curves of LiTDI-PMImTDI and LiTDI-BMImTDI mixtures show similar shape to the LiTDI-EMImTDI one. In their case, though, conductivity values at a given temperature are lower. At 70°C they exhibit ionic conductivity values of 17.3 and 14.6 mS $cm^{-1}$ for P0 and B0, respectively. The same result is initially obtained upon addition of LiTDI, *i.e.* minor decrease in conductivity. In case of PMImTDI, after addition of large fraction of LiTDI, at P37 composition, conductivity reaches 13.3 mS $cm^{-1}$ at 70°C. In case of BMImTDI, conductivity reaches 13.3 mS $cm^{-1}$ at 70°C already at B25 (at the lower concentration of salt). Further addition of LiTDI to PMImTDI results in slow decrease in conductivity (down to 5.2 mS $cm^{-1}$ for P125), until it reaches maximum solubility of 0.15 mole fraction. At this point (P150) ionic conductivity increases up to 12.8 mS $cm^{-1}$ at 70°C. BMImTDI after LiTDI addition to B25 also suffers ionic conductivity decrease, but to a lesser extent. Similarly to LiTDI-PMImTDI mixture, LiTDI-BMImTDI is also subject to the ionic conductivity increase near the LiTDI maximum solubility point - 6.1 mS $cm^{-1}$ for B150 vs. 5.9 mS $cm^{-1}$ for B125, both at 70°C. Ionic conductivity dependence of salt concentration plot shape is similar at all temperatures for a given ionic liquid. Room temperature parameters of the aforementioned points at 20°C for LiTDI-PMImTDI mixtures exhibit conductivities of 3.2, 2.1, 1.5 mS $cm^{-1}$ for P0, P37 and P150, respectively. At 20°C, LiTDI-BMImTDI mixtures show ionic conductivity values of 2.4, 2.2, 1.4 and 0.7 mS $cm^{-1}$ for B0, B25, B50 and B150, respectively.

Recently, such beneficial conductivity plateau (similar to those presented on the Figure 4), have been explained by our group[24] and assigned to ionic associates formation and cation-solvent interactions for LiTDI-solvent systems.

Figure 5 displays the results of viscosity measurements. Shape of the ionic conductivity curve is in agreement with the viscosity plots. As can be easily noticed, the viscosity plots show almost perfect reflecting picture of the conductivity curves. The viscosity plots are also quite interesting, showing almost-plateau areas and even distinct declines in the areas of intermediate local conductivity maxima in all mixtures. Increase of ionic conductivity values in the area of maximum LiTDI solubility (around 0.15 molar fraction) is reflected by drop of viscosity value in case of E150 and P150. Similarly, only slight increase of viscosity in case of B150 takes place instead of typical dynamic increase (geometric growth) at the maximum solubility. Similar behavior can be observed for LiTDI-EMImTDI and LiTDI-PMImTDI mixtures. Starting with 9.1 mPa s at 70°C for E0, viscosity is increasing with the first addition of LiTDI, rising to 11.8 mPa s for E25, then drop to 10.1 mPa s for E37. Further addition of salt causes monotonic viscosity increase up to 16.0 mPa s for E75. Viscosity of EMImTDI mixtures is increasing, though slowly, but for PMImTDI it is descending to 16.4 mPa s at P100. For comparison - P75 exhibits 16.7 mPa s viscosity value. Values at the highest concentrations are almost the same for both ILs – 26.9 and 27.1 mPa s for E125 and P125, as well as 24.0 and 24.4 mPa s for E150 and P150 mixtures, respectively. Viscosity plots of BMImTDI mixtures exhibit smaller number of changes. At 70°C it shows viscosity value of 12 mPa s in case of pure IL (B0). After addition of LiTDI, this value increases to 12.3 mPa s for B12 and 13.3 mPa s for B25. After further additions of LiTDI viscosity value drops to as low as 11.9 mPa s in case of B37 mixture. With the increase of salt fraction in the mixture, viscosity keeps growing monotonically up to the maximum solubility at B150, at which viscosity value is equal to 37.9 mPa s.

Figure 6 shows results of lithium cation transference number ($t_{Li+}$) measurements. Investigated electrolytes offer superior values of $t_{Li+}$ when compared to other ILs.[25,26] The highest measured value is 0.120 for B150, which is indeed an excellent value for good-conducting ILs. For comparison, common values of $t_{Li+}$ for most of state-of-the-art ILs are in the 0.02÷0.04 range.[25] LiTDI-BMImTDI has the highest values of all three presented ILs for LiTDI molar fractions 0.075 and higher. For lower fractions of LiTDI, the best $t_{Li+}$ performance belongs to LiTDI-EMImTDI mixtures, which exhibit $t_{Li+}$ values up to 0.099 (E25). Generally, all ILs mixed with LiTDI are having the same lithium cation transference number plot shapes. They all start with quite low values at 0.0125 LiTDI molar fraction, then after addition to 0.025 molar fraction increase very quickly to reach maxima. Such extrema are absolute maximum in case of LiTDI-EMImTDI and second to value at maximum solubility in case of LiTDI-PMImTDI and LiTDI-BMImTDI. Thus, E25 has the $t_{Li+}$ value of 0.099, P25 - 0.067 and B25 – 0.086. Afterwards, when LiTDI is still added, $t_{Li+}$ values for all ILs are generally decreasing, but reach local maximum at 0.05÷0.075 LiTDI molar fraction ($t_{Li+}$ values: E50 - 0.077, P75 - 0.063 and B75 – 0.065). After reaching global minimum at 0.1 molar fraction, the $t_{Li+}$ values are increasing upon further LiTDI salt addition to obtain at maximum solubility - 0.15 molar fraction – maxima. These maxima are global for P and B mixtures – 0.093 and 0.120, for P150 and B150, respectively - and local for E mixtures – 0.040 for E150). The $t_{Li+}$ and ionic conductivity values usual relationship is more-less reciprocal. What is uncommon in the presented mixtures is combined increase of both these quantities at low LiTDI concentrations and at the maximum solubility of LiTDI. It means the possibility to obtain the highest values of cell-usable conductivity – lithium cation conductivity, $\sigma_{Li+}$. This quantity is obtained by multiplying values of lithium cation transference number and ionic conductivity at the same concentration. Thus, top values of

lithium cation conductivity can be found at low salt concentrations: E25, P37, B25, as well as at the maximum solubility (E150, P150, B150).

These three phenomena – ionic conductivity plots with high retained conductivity upon lithium salt addition, uncommon ionic conductivity-viscosity and ionic conductivity-cation transference number relations – can be explained by the special, "tailored" structure of the TDI anion. It was especially dedicated for electrolyte applications, which was designed to have the lowest possible coordinating properties, *i.e.* uniformed charge distribution, weakened ionic interactions. Use of the same anion in lithium salt and in IL may also result in specific interactions between salt and a solvent. Especially interesting is the viscosity decline at the maximum solubility point, which is, also worth to note, at the same molar fraction for all ILs. It was, to our best knowledge, never seen before combined together with high transference number, as in mixtures presented herein. Our assumption is that, due to the earlier findings,[27-30] the maximum solubility ratio is defined by ratio at which lithium cation is fully solvated by the IL anions. In that case there are two possibilities. One is that 1:6 ratio (0.143 molar fraction of LiTDI in IL) is the effect of coordinating lithium by six anions, which was suggested by some researchers.[31] This is less probable assumption due to our structural findings presented herein - in case of nitrogen ligation centers, coordinating number of the lithium cation is four (see below), which is in concert with other works.[27,29] If it would be fully coordinated, then for every one lithium cation there are four anions coordinated with it [$Li(TDI)_4^{3-}$] through a direct bonding and three TDI anions and six IL cations not coordinated directly. As it was shown many times before, IL ions are usually forming agglomerates and it is quite common for them to exist in the form of triplets - of $C_2A^+$ and $CA_2^-$ type. Hence, it would be probable for them to be in such a form also in the mixtures presented here and to form triplets of, *e.g.* $EMIm_2TDI^+$ form, keeping the whole electrolyte neutral in the charge terms. Then the 1:6 ratio of saturated LiTDI-IL mixture (0.143 LiTDI molar fraction) would

be a result of 1:4 coordinated lithium cation and the rest of cations and anions would be forming the triplet type agglomerates. Such agglomerates would be more immobile than individual ions and as such, giving the lithium cation a chance to have higher transference number as well as relatively better mobility. As a result, lower viscosity and higher ionic conductivity would be achieved.

Crystallographic analyses were performed on the EMImTDI pure IL, as well as LiTDI-PMImTDI and LiTDI-BMImTDI complexes. The crystallographic details can be found in the Electronic Supplementary Information (ESI). Single crystals of EMImTDI were obtained by recrystallization from methanol solutions. Single crystals of compounds LiTDI-PMImTDI and LiTDI-BMImTDI suitable for X-ray diffraction analysis were grown at room temperature from a $LiTDI_{0.5}PMImTDI_{0.5}$ and $LiTDI_{0.5}BMImTDI_{0.5}$.composition. X-Ray crystal structure determination of EMImTDI, reveals planar layers of cations and anions interacting through hydrogen bonds (Figure 7).

The TDI anion makes four in-plane hydrogen bonds to methylene hydrogen atoms of cations at the C9, C10 and C11 positions. Namely, a short, bifurcated contact between the hydrogen atom at C10 and N1/F3 atoms, a hydrogen bond between H9 and imidazole nitrogen atom N2, and short contact methylene hydrogen atom H11 and nitrile nitrogen N4. The layers are stacked one above the other in the ABAB fashion through ionic interactions between cations and anions from adjacent layers.

Lithium electrolytes formed by addition of LiTDI salt to PMImTDI (**2**) and BMImTDI (**3**) ILs crystallize in the triclinic space group $P\bar{1}$ as colorless plates. In both cases, single crystal X-ray analysis showed a novel 1D ladder-like assembly of the $[Li(TDI)_2]_n^{n-}$ polyanions as depicted in Figure 8.

Lithium cations adopt distorted tetrahedral geometry and are linked via two bridging dicyanoimidazolato ligands forming characteristic dimeric units with ten-membered

$Li(NCCN)_2Li$ ring.[32] The central ring is planar with r.m.s. deviations from planarity of 0.012 Å for both **2** and **3**. Dimeric units are linked to each other through the spanning TDI anions which are coordinated in an unsymmetrical fashion through the nitrogen atom of the imidazole ring and one of the cyano groups. Consequently, the ladder-like 1D coordination polymer propagate in the direction of the *X* axis, with the Li−Li distance along the chain being equal to the *a* cell parameter, 8.2837(2) and 8.4241(1) Å for **2** and **3** respectively. Polyanions are arranged in column-type fashion with perpendicular channels occupied by imidazolium cations as shown in Figure 9.

Coordination polymers in structures **2** and **3** are characteristic and consistent with observations made by Henderson[31] for LiTFSI-xMImTFSI system (coordination number = 6). It is worth stressing that in case of LiTDI-xMImTDI system coordination sphere is completely different, due to the presence of nitrogen donor centers. Coordination number in our case is 4 (with one additional fluorine dative bond). Unlike LiTFSI-xMImTFSI, in case of LiTDI-xMImTDI system TDI anion enforce formation of dimeric moieties ($Li_2TDI_2$) which are subsequently linked via bridging TDI anionic ligands.

That allows implying that addition of the IL effects in this coordination polymer $[Li(TDI)_2^{n-}]$ dissociation. At first, due to coordination polymer interaction with TDI anions, the dimeric structure is retained after fulfilling the coordination sphere. As the effect of that we assume formation of $Li_2TDI_6^{4-}$ species (double triplets). Unusual conductivity plot could be a consequence of existence of such dimers in more concentrated solution. During further dissolution one might expect occurrence of equilibria with lithium mononuclear complexes $LiTDI_4^{3-}$.

Noteworthly, almost identical crystal structures are observed for different organic cations. That fact proves stability of the anionic coordination polymers formed. Thus, the

observed crystal structure assembly of the described species is directed by acidic lithium center interacting with TDI anions.

## 4. Conclusions

We have presented the three new ILs that are based on our anion "tailored" for electrochemical applications: EMImTDI, PMImTDI and BMImTDI. All three ILs are thermally and electrochemically stable. They also contain less fluorine than industry standard ($PF_6^-$), which is bound in more stable way than with P-F or B-F bonds. Lithium electrolytes formed by the addition of LiTDI salt to these ILs reach high ionic conductivity - over 3 mS at 20°C. New IL-based electrolytes exhibit good lithium cation transference numbers (over 0.1) overlapping with high ionic conductivity. Negligible change of the ionic conductivity upon lithium salt addition (less than 10% instead of few-fold decrease)[33] combined with high ionic conductivity was never seen before. As a result, we introduce safe, effective and in many aspects environmentally friendly completely new class of electrolytes.

## Acknowledgements

This work was financially supported by Warsaw University of Technology.

This work has been supported by the European Union in the framework of European Social Fund through the Warsaw University of Technology Development Programme, realized by Center for Advanced Studies.

## Figures

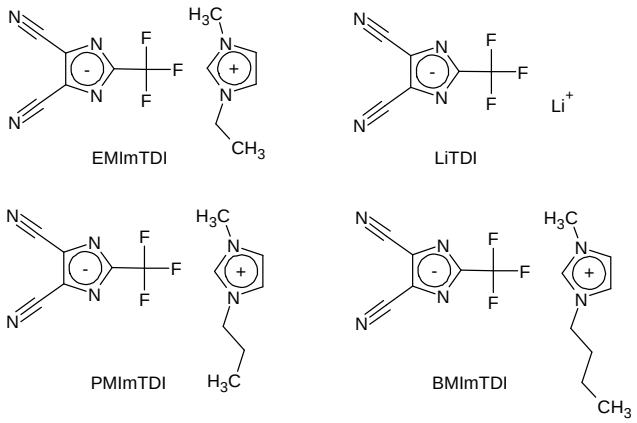


Fig. 1. Structural formula of LiTDI salt and ionic liquids: EMImTDI, PMImTDI and BMImTDI.

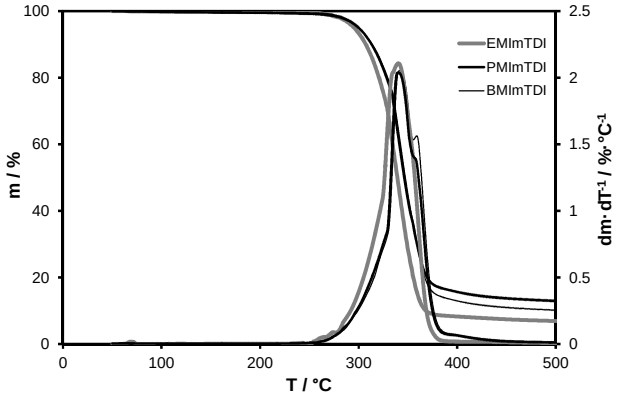


Fig. 2. Thermogravimetric analysis TGA and DTG plots of EMImTDI, PMImTDI and BMImTDI.

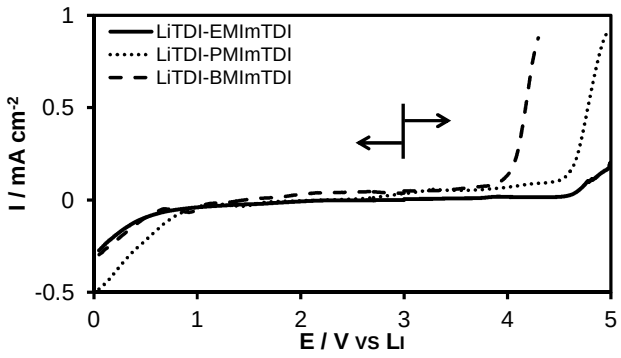


Fig. 3. Linear sweep voltammetry plots for $LiTDI_{0.1}EMImTDI_{0.9}$, $LiTDI_{0.1}PMImTDI_{0.9}$, and $LiTDI_{0.1}BMImTDI_{0.9}$ mixtures with platinum as working electrode and lithium metal electrode as reference, all experiments performed with 1 mV $s^{-1}$ scan rate.

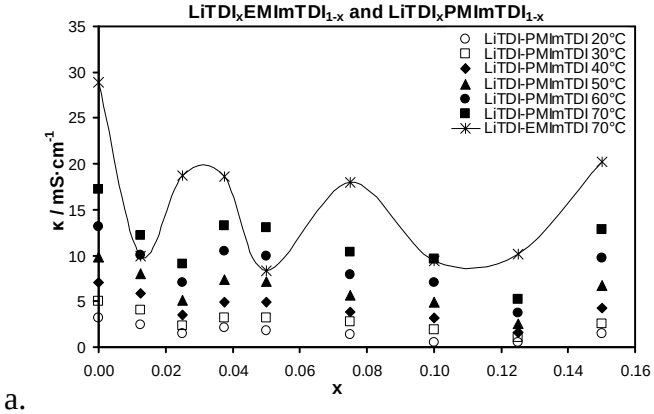


a.

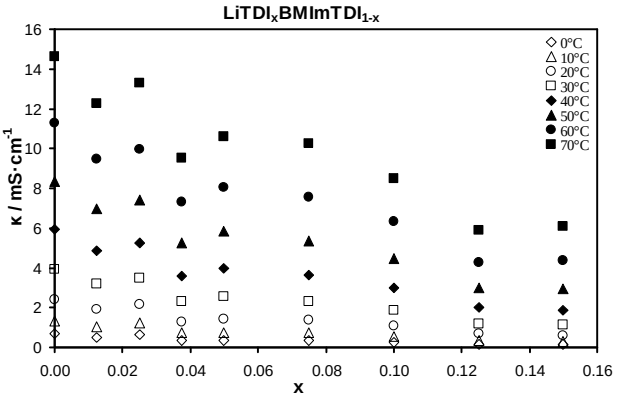


b.

Fig. 4 Ionic conductivity dependence of LiTDI content in a. LiTDI-EMImTDI mixture at 70°C and in LiTDI-PMImTDI mixture in 20÷70°C temperature range, line is used only to guide the eye; b. LiTDI-BMImTDI mixture in 0÷70°C temperature range.

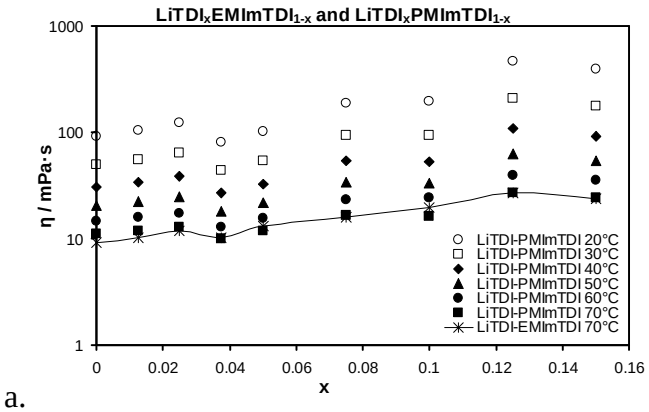


a.

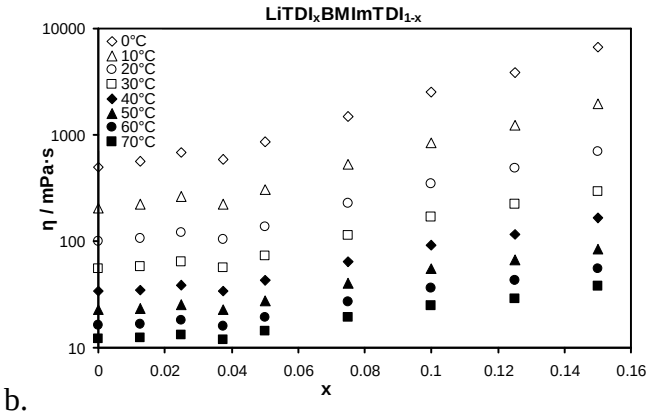


b.

Fig. 5. Viscosity dependence of LiTDI content in a. LiTDI-EMImTDI mixture at 70°C and in LiTDI-PMImTDI mixture in 20÷70°C temperature range, line is used only to guide the eye; b. LiTDI-BMImTDI mixture in 0÷70°C temperature range.

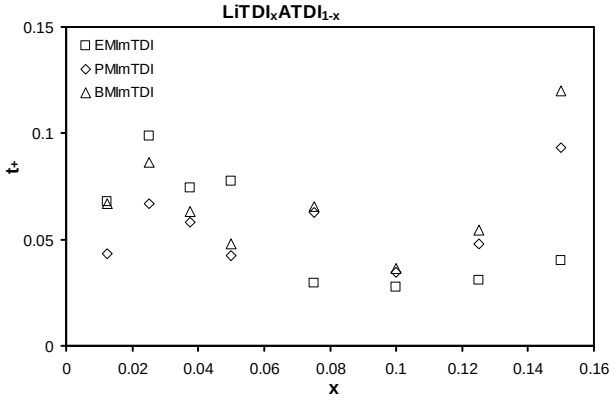


Fig. 6. Lithium cation transference number dependence of LiTDI content in LiTDI-EMImTDI mixture at 70°C, in LiTDI-PMImTDI mixture at ambient temperature and in LiTDI-BMImTDI mixture at ambient temperature. All values were averaged over three samples.

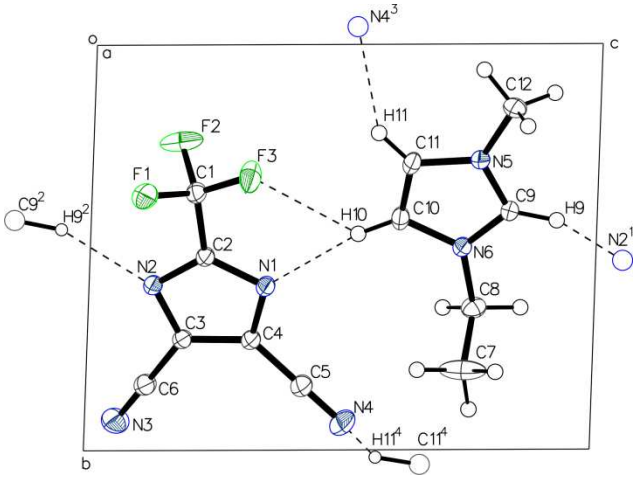


Fig. 7. Thermal ellipsoid plot of ions in the EMImTDI asymmetric unit with atom numbering scheme and hydrogen bonds motif constituting individual layers. H···*A* distance: H9···N2$^{1}$ 2.40 Å; H10···F3 2.49 Å; H10···N1 2.35 Å; H11···N4$^{3}$ 2.57 Å. Symmetry codes: ($^{1}$) +*x*,+*y*,1+*z*; ($^{2}$) +*x*,+*y*, −1+*z*; ($^{3}$) 1+*x*, −1+*y*,+*z*; ($^{4}$) −1+*x*,1+*y*,+*z*.

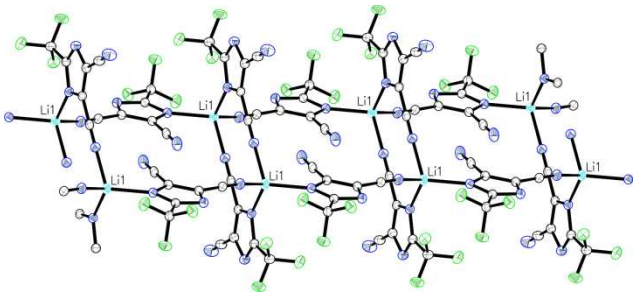


Fig. 8. Perspective view of the ladder-like polyanionic $[Li(TDI)_2]_n^{n-}$ chain observed in the crystal structure of **2** (LiTDI-PMImTDI) and **3** (LiTDI-BMImTDI).

a.

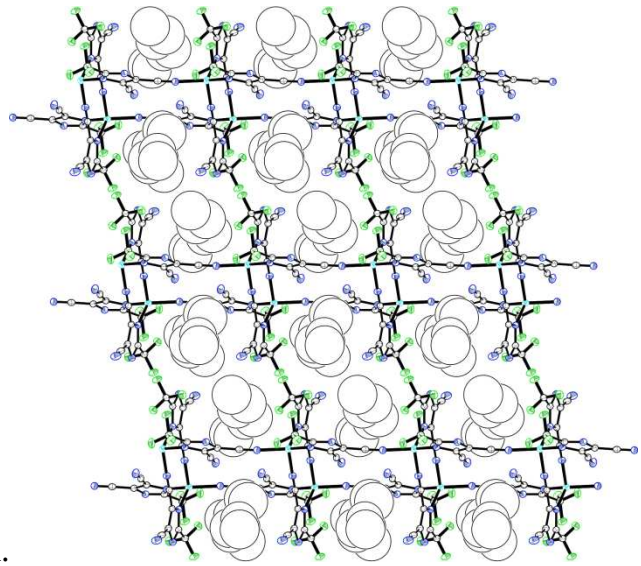

b.

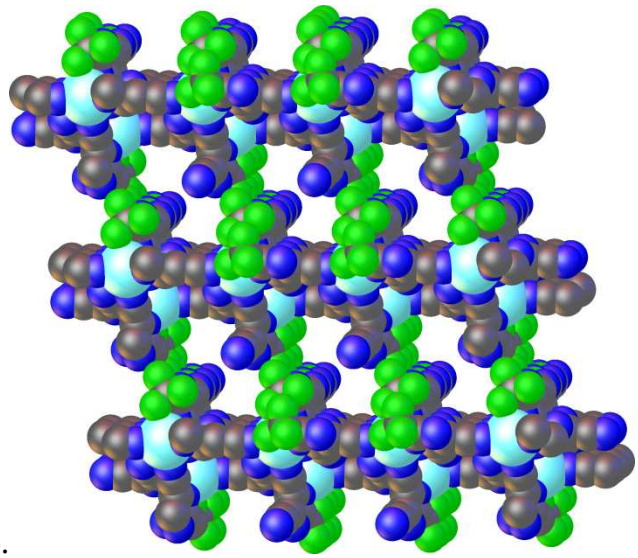

Fig. 9. Ion packing in the crystal structure of **3** (LiTDI-BMImTDI): a. Presentation of the channels occupied by imidazolium cation molecules shown in space-filling mode, view along the *b*-axis; b. Space-filling model of three-dimensional formation of the channels. Color code: gray C; green: F, blue: N, cyan: Li.

## References


1. M. Armand and J.-M. Tarascon, *Nature*, 2008, **451**, 652.

2. B. Scrosati, J. Hassoun and Y. K. Sun, *Energy Environ. Sci*. 2011, **4**, 3287.

3. V. Etacheri, R. Marom, R. Elazari, G. Salitra, D. Aurbach, *Energy Environ. Sci.*, 2011, **4**, 3243.

4. M. Egashira, B. Scrosati, M. Armand, S. Béranger, C. Michot, *Electrochem. Solid-State Lett.*, 2003, **6**, A71.

5. L. Niedzicki, M. Kasprzyk, K. Kuziak, G.Z. Żukowska, M. Armand, M. Bukowska, M. Marcinek, P. Szczeciński, W. Wieczorek, *J. Power Sources*, 2009, **192**, 612.

6. L. Niedzicki, M. Kasprzyk, K. Kuziak, G.Z. Żukowska, M. Marcinek, W. Wieczorek, M. Armand, *J. Power Sources*, 2011, **196**, 1386.

7. L. Niedzicki, S. Grugeon, S. Laruelle, P. Judeinstein, M. Bukowska, J. Prejzner, P. Szczecinski, W. Wieczorek, M. Armand, *J. Power Sources*, 2011, **196**, 8696.

8. *World Pat.*, 023 413, 2010, *Fr. Pat.*, 2 935 382, 2009.

9 D.W. McOwen, S.A. Delp, W.A. Henderson, Meeting Abstracts 2013, MA2013-02, 1182.

10. P. Ribiere, S. Grugeon, M. Morcette, S. Boyanov, S. Laruelle, G. Marlair, *Energy Environ. Sci.*, 2012, **5**, 5271.

11. R. Renner, *Environ. Sci. Technol.*, 2001, **35**, 410A.

12. A.E. Visser, R.P. Swatloski, W.M. Reichert, R. Mayton, S. Sheff, A. Wierzbicki, J.H. Davis, R.D. Rogers, *Environ. Sci. Technol.*, 2002, **36**, 2523.

13. U. Domańska, in *General review of ionic liquids and their properties* in *Ionic Liquids in chemical analysis*, ed. M. Koel, CRC Press Taylor&Francis Group, ch. 1.

14. J.P. Hallet, T. Welton, *Chem. Rev.*, 2011, **111**, 3508.

15. N. Plechkova, K. Seddon, *Chem. Soc. Rev.*, 2008, **37**, 123.

16. M. Armand, F.Enders, D. MacFarlane, H.Ohno, B. Scrosati, *Nat. Mater.*, 2009, **8**, 621.

17. A. Fernicola, F. Croce, B. Scrosati, T. Watanabe, H. Ohno, *J. Power Sources*, 2007, **174**, 342.

18. L. Niedzicki, G.Z. Żukowska, M. Bukowska, P. Szczeciński, S. Grugeon, S. Laruelle, M. Armand, S. Panero, B. Scrosati, M. Marcinek, W. Wieczorek, *Electrochim. Acta*, 2010, **55**, 1450.

19. CRYSALIS$^{PRO}$ Software system, Agilent Technologies UK Ltd., Oxford, UK, 2012.

20. G. M. Sheldrick, *Acta Crystallogr., Sect. A: Found. Crystallogr*., 2008, ***64***, 112.

21. O. V. Dolomanov, L. J. Bourhis, R. J. Gildea, J. A. K. Howard and H. Puschmann, OLEX2: A complete structure solution, refinement and analysis program. *J. Appl. Cryst*. 2009, *42*, 339.

22. P. Bruce, C. Vincent, *J. Electroanal. Chem*. 1987, **225**, 1.

23. A. Chowdhury, S.T. Thynell, *Thermochim. Acta*, 2006, **443**, 159.

24. L. Niedzicki, E. Karpierz, A. Bitner, M. Kasprzyk, G.Z. Zukowska, M. Marcinek, W. Wieczorek, *Electrochim. Acta*, 2014, **117C**, 224.

25. K. Hayamizu, Y. Aihara, H. Nakagawa, T. Nukuda, W.S. Price, *J. Phys. Chem. B*, 2004, **108**, 19527.

26. T. Frömling, M. Kunze, M. Schönhoff, J. Sundermeyer, B. Roling, *J. Phys. Chem. B*, 2008, **112**, 12985.

27. O. Borodin, G.D. Smith, W. Henderson, *J. Phys. Chem. B*, 2006, **110**, 16879.

28. J. Pitawala J.-K. Kim, P. Jacobsson, V. Koch, F. Croce, A. Matic, *Faraday Discuss.*, 2012, **154**, 71.

29. J. Scheers, J. Pitawala, F. Thebault, J.-K. Kim, J.-H. Ahn, A. Matic, P. Johansson, P. Jacobsson, *Phys. Chem. Chem. Phys.*, 2011, **13**, 14953.

30. P.M. Dean, J.M. Pringle, D.R. MacFarlane, *Phys. Chem. Chem. Phys.*, 2010, **12**, 9144.

31. Q. Zhou, K. Fitzgerald, P.D. Boyle, W.A. Henderson, *Chem. Mater*, 2010, **22**, 1203.

32. M. Dranka, L. Niedzicki, M. Kasprzyk, M. Marcinek, W. Wieczorek, J. Zachara, *Polyhedron*, 2013, **51**, 111.

33. A. Lewandowski, A. Świderska-Mocek, *J. Power Sources*, 2009, **194**, 601.